13th Australasian Fluid Mechanics Conference
Monash University, Melbourne, Australia
13-18 December 1998

FUNDAMENTAL STUDIES OF A SYNTHETIC JET ACTUATOR

S.G. MALLINSON, G. HONG and J.A. REIZES

Faculty of Engineering
University of Technology Sydney, Broadway, NSW, AUSTRALIA

ABSTRACT

The flow generated by a synthetic jet actuator is investigated experimentally and computationally. The experimental data and computational predictions show good agreement with the theory for a steady turbulent jet. It is found, however, that the synthetic jet establishes itself much more rapidly than the steady jet, and this is thought to be the result of turbulent dissipation causing a vortex to be trapped near the actuator orifice. Also, the optimal forcing frequency was found to be in agreement with a coupled fluid-structural interaction model.

INTRODUCTION

Micro-electro-mechanical systems (MEMS) are a novel concept which can be used to control large-scale flow features, such as separation, transition and mixing. MEMS couple sensors, control and logic electronics and actuators into a single compact device. The actuators are used to introduce disturbances whose characteristic scales are similar to or smaller than the actual flow features. Potential actuators for MEMS applications include the micro-flap (Naguib et al., 1997), the cantilever-cavity actuator (Jacobson and Reynolds, 1998) and the synthetic jet (Smith and Glezer, 1997), the latter being the focus of the present study.

The synthetic jet actuator consists of an electrically-oscillated membrane located at the bottom of a small cavity which has an orifice in the face opposite the membrane (see Figure 1). During one cycle, fluid is expelled through the orifice as the membrane moves upwards. This induces a vortex ring at the edge of the orifice due to flow separation. The vortex ring then moves outwards under its own momentum. When the membrane moves downwards, air is entrained into the cavity. Ideally, the vortex ring is sufficiently distant from the orifice so that it is not influenced by the entrainment of fluid into the cavity. Over a single period of oscillation of the membrane, there is, therefore, zero net mass-flux into or out of the cavity, yet there is a non-zero mean jet velocity (Smith and Glezer, 1997). Flow control has previously been achieved using (traditional) steady jets. The obvious benefit to employing synthetic jets is that they require no air supply and so there is only a minor weight penalty compared with that due to the piping, connections and compressors associated with steady jets.

Even though synthetic jets have recently been employed for a number of flow control applications (delaying transition (Lorkowski et al., 1997), delaying separation (Sinha and Pal, 1993; Amitay et al., 1998), improving mixing (Smith and Glezer, 1997)), there has been only a few in depth investigations of their operation. Smith and Glezer (1997) noted that the jets exhibit a standing vortex near the exit, in contrast to the ideal flow picture shown in Figure 1. This was explained as being due to turbulent dissipation of the vortex cores. They also noted that the flow was established closer to the orifice than for a steady jet. Kral et al. (1997) found numerical simulations of synthetic jet flow to be in better agreement with the data of Smith and Glezer when the flow was assumed to be fully turbulent. Rathnasingham and Breuer (1997) developed a coupled fluid-structure interaction model for synthetic jet actuators. From this, the optimum forcing frequency could be determined for a given set of actuator geometric parameters and structural properties. Good agreement was observed between this theory and a limited set of experimental data.

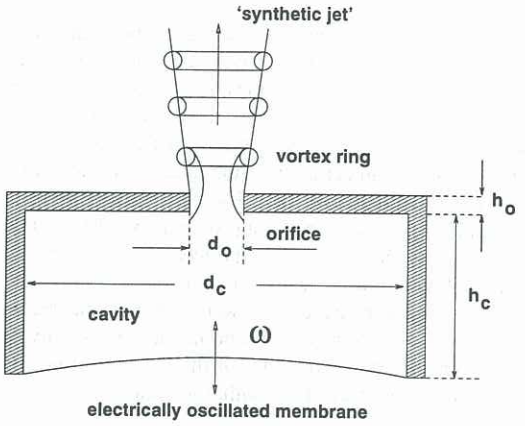

Figure 1 : Schematic diagram of a synthetic jet actuator. d_o = orifice diameter, d_c = cavity diameter, h_o = orifice height, h_c = cavity height, ω = forcing frequency.

Here, an individual synthetic jet is investigated using both experimental and computational methods. In particular, this study examines why the flow is established closer to the orifice than a steady jet and whether or not the theory of Rathnasingham and Breuer (1997) is valid for conditions different to those examined in their paper.

EXPERIMENTAL METHOD

The technology for the sensors and electronics aspects of MEMS is relatively mature (Ho and Tai, 1996). MEMS are normally manufactured using micromachining of silicon, which allows sensors and electronics to be integrated into the design process from the beginning. This study is not concerned with the fabrication of MEMS so that a simple version of the actuator, which does not rely on any micromachining processes, is employed here. This is consistent with previous studies that have investigated the application of such devices (see, for example, Lorkowski et al. (1997)). In this way, it is easy to manufacture the actuators and to modify their geometric parameters.

The actuator membrane is a brass shim, firmly clamped at its perimeter, with a natural frequency of approximately 1.45 kHz. Forcing is achieved using a piezoceramic disc bonded to the lower surface of the membrane. The input to the piezoceramic is supplied by a signal generator. All tests were conducted using an input sinusoidal signal with ω =1.45 kHz. The geometric parameters of the actuator are: h_c = 1.15 mm, d_c = 40 mm, h_o = 1.65 mm and d_o = 0.75 mm (see Figure 1).

The jet velocity was measured using single-component hot wire anemometry (Bruun, 1995). The sample rate was set at 20 kHz and 131072 samples were acquired for each record. Each measurement was repeated at least five times and average values were obtained from these. It is estimated that the uncertainty in the mean and fluctuating velocity measurements was < ±1%. Measurements made at distances greater than approximately 20 orifice diameters from the orifice were noticeably susceptible to small amplitude motions caused by air fluctuations in the laboratory. These measurements were not as repeatable as those made closer to the orifice and had an uncertainty of ±3%. To check the axisymmetry of the jet, measurements were made at a number of azimuthal orientations.

COMPUTATIONAL METHOD

Unsteady incompressible numerical simulations were performed using a commercially available Navier-Stokes solver called CFX4.2. It employs a finite-volume formulation and the simulations can assume either laminar or turbulent flow, the latter computed using the k-ε model (Launder and Sharma, 1974). The flow was assumed to be axisymmetric with the symmetry plane lying along the jet centre-line.

A computational mesh with 201 nodes in the stream-wise direction and 110 nodes in the transverse direction was employed here. Computations with meshes having half the number of cells exhibited only small differences (1% or less), indicating that mesh convergence has been achieved. The computational domain extends 32 mm in the stream-wise direction and 12.75 mm in the transverse direction. The mesh is refined near the edge of the orifice.

Following Kral et al. (1997), the actuator is modeled as a boundary condition for the velocity normal to the orifice opening:

$$u_n(t) = U_o \sin(\omega t) \qquad (1)$$

where U_o is the forcing velocity. That is, the cavity flow is not considered. The value of U_o is varied and for the present study, the best agreement with experiment was achieved for U_o = 30 m s^{-1}.

RESULTS and DISCUSSION

The measured and computed centre-line distribution of the synthetic jet mean velocity, u_c, are compared in Figure 2. Also shown is the measured centre-line distribution of the fluctuating component of velocity, u'. Both u_c and u' are seen to fall rapidly with distance from the orifice, with the fluctuating component decreasing more rapidly for $y / d_o > 5$. For the mean velocity, good agreement is observed between experiment and computation for $y / d_o > 15$. Closer to the orifice, there is a large discrepancy. This may be due to there being

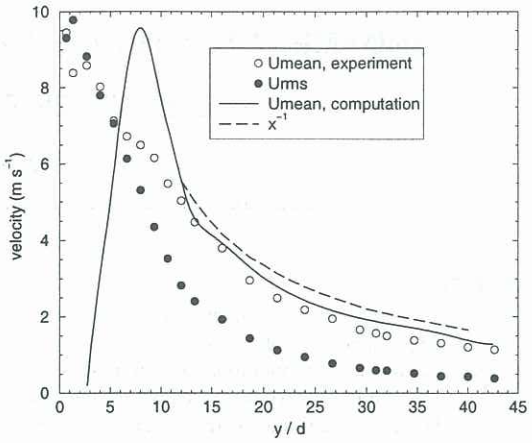

Figure 2. Jet centre-line velocity.

insufficient mesh points in the near orifice region. It may also be that the flow near the orifice is not accurately modeled using the current boundary condition. Kral et al (1997) also predicted the mean velocity along the centre-line to peak before decaying. However, they did not have any data with which to compare their computations for $y / d_o < 10$. It may be, therefore, that a computation of the complete flow-field, including the cavity interior, is required to accurately model this region. Another possibility is that the size of the hot-wire probe is too large to correctly measure the flow near the orifice, and that either smaller probes or another technique (such as laser-doppler anemometry) must be used in this region. We plan to explore all three of these possibilities in future studies.

Also shown in Figure 1 is a curve representing the expected variation of the centre-line velocity for a steady axisymmetric turbulent jet, that is y^{-1} (Rajaratnam, 1976). The experiment and computation are both seen to vary as y^{-1} for $y / d_o > 12$, indicating that the flow becomes self-similar after approximately 12 orifice diameters. This contrasts with the steady jet for which self-similar flow is not established until approximately 40 orifice diameters (Rajaratnam, 1976). A similar observation was made by Smith and Glezer (1997).

The measured and predicted profiles of mean velocity are shown in Figure 3 for five stream-wise stations: y / d_o = 4, 8, 12, 18.7 and 26.7. The velocity data are normalized by u_c and the transverse direction, x, is normalized by the value of the full-width at half-maximum, b. The profiles exhibit a strong peak near the centre-line and fall away with distance from the orifice. Also shown is the theoretical Tollmein solution for a steady axisymmetric turbulent jet (Rajaratnam, 1976). All the data and computations collapse reasonably well implying that the flow is self-similar for $y / d_o > 4$, which is much earlier than is indicated by the centre-line velocity distributions (Figure 2).

The profiles of fluctuating velocity are presented in Figure 4. Close to the orifice, the profiles show a strong central peak. As y / d_o increases, the maximum decreases and the profiles become flatter in the central region of the jet. This would appear to suggest that the turbulence induced by the synthetic jet spreads outwards as the flow proceeds away from the orifice and that self-similar flow

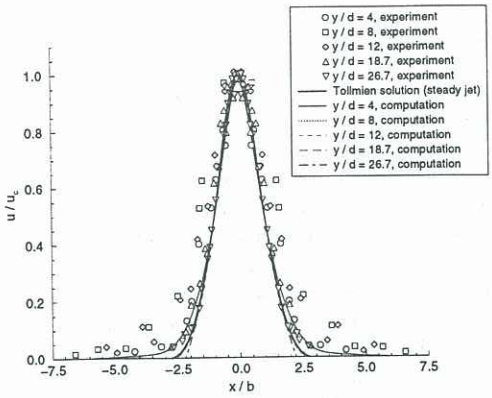

Figure 3. Jet mean velocity profiles.

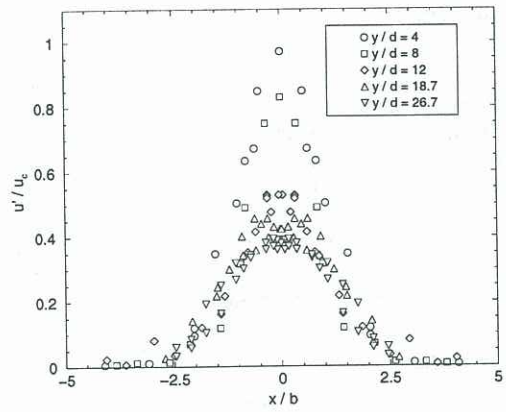

Figure 4. Jet fluctuating velocity profiles.

is achieved for $y / d_o > 12$, consistent with Figure 2. It would seem, therefore, that the mean velocity profiles (see Figure 3) are a less sensitive indicator of similarity than the fluctuating velocity profiles.

Figure 5 shows a time sequence of vorticity contour plots which were computed assuming turbulent flow. The non-dimensional time is defined as $t^* = t\ U_o / d_o$, where t is the physical time. The first vortex moves away from the orifice after it has emerged from the orifice. It merges with the vortex which follows and its rate of migration away from the orifice is very slow. It appears that the subsequent vortices are 'trapped' just near the orifice. Figure 6 shows a contour plot for a much later time, $t^* =$ 600. The primary vortex still lies close to orifice. We performed simulations with higher values of the forcing velocity and found that this caused the primary vortex to be situated further from the orifice. Presumably, for a sufficiently large value of U_o, the vortex momentum would be able to overcome the effect of turbulent dissipation and break away, producing a flow pattern similar to that shown in Figure 1. Figure 7 shows a contour plot for a laminar computation for the present actuator at $t^* = 96$. Note the expanded scales in the transverse and stream-wise directions. Here, there is no turbulent dissipation and the flow pattern bears a strong resemblance to the idealized pattern shown in Figure 1.

The effect of turbulence seems to be an increased dissipation of energy which reduces the rate of spread of the vortices. Thus, the vortices are smaller for the turbulent flow and they move away from the orifice more slowly. For the laminar flow, at $t^* = 96$, the diameter of

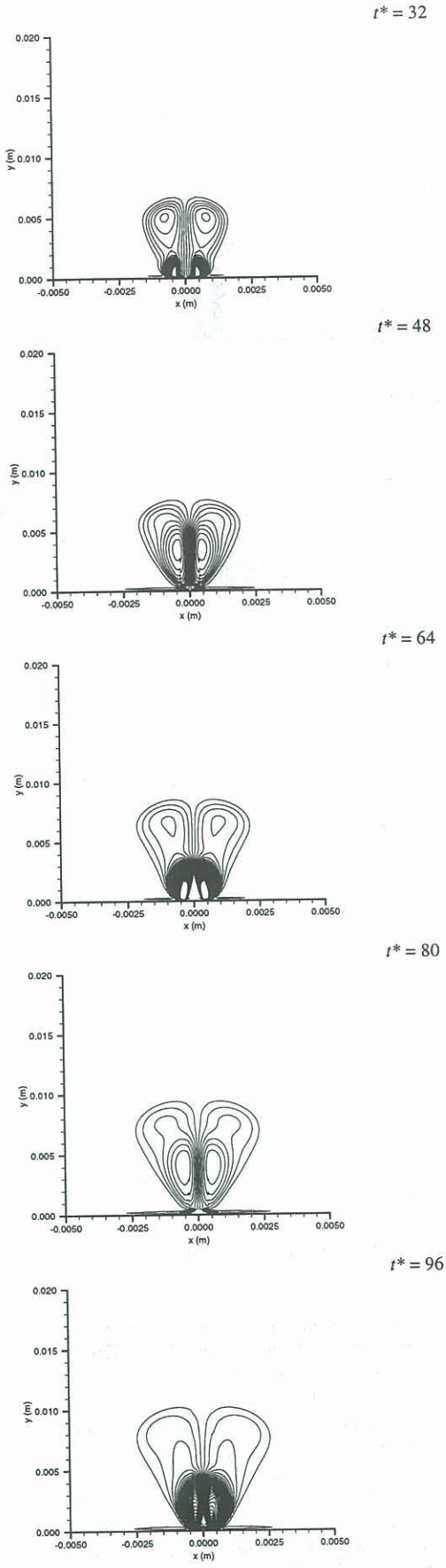

Figure 5. Time sequence of vorticity contours, turbulent simulation.

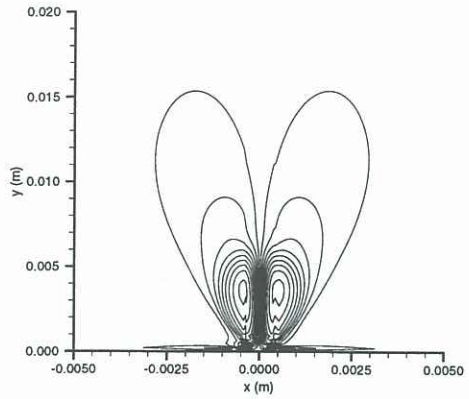

Figure 6. Vorticity contours, for $t^* = 600$, turbulent simulation.

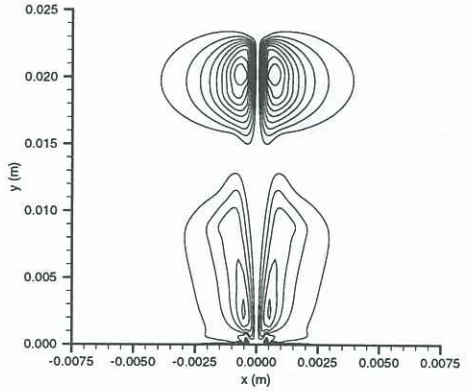

Figure 7. Transverse velocity contours, laminar simulation, $t^* = 96$.

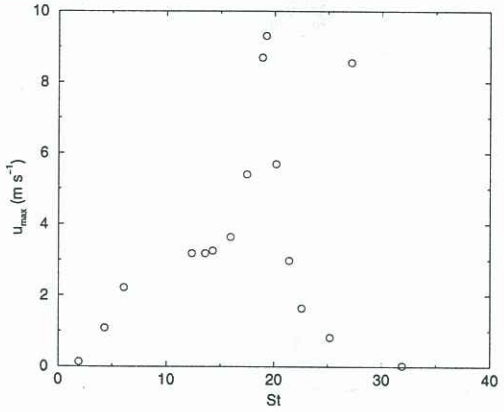

Figure 8. Maximum jet velocity of a function of Stokes parameter.

the first vortex to emerge is approximately 8 mm and its centre lies nearly 20 mm from the orifice. For the turbulent flow at $t^* = 96$, the diameter is 5 mm and the location is 8 mm. Further, for the turbulent simulation there is an oscillating flow near the orifice which means that the primary vortex is trapped. A jet flow is forced through the centre of this vortex, which also limits the size of the turbulent core near the orifice. This would explain why the synthetic jet appears to establish itself much more quickly than a steady jet, whose core is free to grow.

Rathnasingham and Breuer (1997) present a theory for determining the synthetic jet membrane forcing frequency that, for a given set of geometric and structural characteristics, will produce the largest jet velocity. For the present actuator, this theory predicts the optimum frequency, expressed in terms of the Stokes parameter, $St = (\omega\, d^2/\nu)^{1/2}$, to be approximately 19. Figure 8 presents the maximum jet velocity, measured on the centre-line at $y / d_o = 1$, for a range of Stokes parameters (frequencies). The same forcing voltage was used in each case. There is a strong peak near $St = 19$, at the natural frequency of the membrane, $\omega = 1.45$ kHz, in agreement with theory. There is also a second peak near $St = 27$ and this corresponds to the second harmonic. No other peaks were found for $St < 1000$.

CONCLUSION

The flow produced by a synthetic jet actuator has been examined. Experimental data and computational predictions are in good agreement with each other and with the theory for a steady turbulent jet. It is seen, however, that the synthetic jet establishes itself more rapidly than a steady jet. This seems to be caused by turbulent dissipation, which traps a vortex near the orifice, thus limiting the size of the turbulent core. The optimum forcing frequency is in good agreement with the theory of Rathnasingham and Breuer (1997).

REFERENCES

AMITAY, M., SMITH, B.L. and GLEZER, A., "Aerodynamic flow control using synthetic jet technology," *AIAA paper* 98-0208, 1998.

BRUUN, H.H, *Hot-Wire Anemometry*, Oxford Science, 1995.

HO, C.-M. AND TAI, Y.-C., "Review: MEMS and its applications for flow control," *ASME J. Fluids Eng.*, **116**, 437-447, 1996.

JACOBSON, S.A. and REYNOLDS, W.C., "Active control of streamwise vortices and streaks in boundary layers," *J. Fluid Mech.*, **360**, 179-211, 1998.

KRAL, L.D., DONOVAN, J.F., CAIN, A.B. and CARY, A.W., "Numerical simulations of synthetic jet actuators," *AIAA paper* 97-1824, 1997.

LAUNDER, B.E. AND SHARMA, B.I., "Turbulence models and their application to the prediction of internal flows," *Letts. Heat and Mass Transf.*, **1**, 131-138, 1974.

LORKOWSKI, T., RATHNASINGHAM, R. AND BREUER, K.S., "Small-scale forcing of a turbulent boundary layer," *AIAA paper* 97-1792, 1997.

NAGUIB, A., CHRISTOPHOROU, C., ALNAJJAR, E., NAGIB, H., HUANG, C.C. and NAJAFI, K., "Arrays of MEMS-based actuators for control of supersonic jet screech," *AIAA paper* 97-1963, 1997.

RAJANATNAM, N., *Turbulent Jets*, Elsevier, 1976.

RATHNASINGHAM, R. and BREUER, K.S., "Coupled fluid-structural characteristics of actuators for fluid control," *AIAA J.*, **35**, 832-837, 1997.

SINHA, S.K. and PAL, D., "On the differences between the effect of acoustic perturbation and unsteady bleed in controlling flow separation over a circular cylinder," *SAE Tech. Paper* 932573, 1993.

SMITH, B.L. AND GLEZER, A., "Vectoring and small-scale motions effected in free shear flows using synthetic jet actuators," *AIAA paper* 97-0213, 1997.